



Comparative study of bilateral putamen for patients with severe Parkinson's disease detected by ¹H magnetic resonance spectroscopy

Biao Qu¹, Xiaoyuan Li², Min Xiao³, Runhan Chen⁴, Hejuan Tan³, Hongwei Sun⁵, Rushuai Li², Jingjing Xu⁶, Jiyang Dong⁶, Gaofeng Zheng¹, Shuyue Ai^{2#}, Xiaobo Qu^{6#}

¹Pen-Tung Sah Institute of Micro-Nano Science and Technology, Xiamen University, Xiamen, China; ²Department of Nuclear Medicine, Nanjing First Hospital, Nanjing Medical University, Nanjing, China; ³Institute of Artificial Intelligence, Xiamen University, Xiamen, China; ⁴National Institute for Data Science in Health and Medicine, Xiamen University, Xiamen, China; ⁵United Imaging Research Institute of Intelligent Imaging, Beijing, China; ⁶Biomedical Intelligent Cloud R&D Center, Fujian Provincial Key Laboratory of Plasma and Magnetic Resonance, Department of Electronic Science, Xiamen University, Xiamen, China

Contributions: (I) Conception and design: B Qu, S Ai, X Qu; (II) Administrative support: G Zheng, X Qu; (III) Provision of study materials or patients: X Li, R Li, S Ai; (IV) Collection and assembly of data: B Qu, X Li, R Li; (V) Data analysis and interpretation: B Qu, J Xu, J Dong, M Xiao, H Tan; (VI) Manuscript writing: All authors; (VII) Final approval of manuscript: All authors.

#These authors contributed equally to this work.

Correspondence to: Shuyue Ai, MM. Department of Nuclear Medicine, Nanjing First Hospital, Nanjing Medical University, 68 Changle Road, Nanjing 210006, China. Email: asy331@sina.com; Xiaobo Qu, PhD. Biomedical Intelligent Cloud R&D Center, Fujian Provincial Key Laboratory of Plasma and Magnetic Resonance, Department of Electronic Science, Xiamen University, 422 Siming South Road, Xiamen 361005, China. Email: quxiaobo@xmu.edu.cn.

Background: The diagnosis of Parkinson's disease (PD) is challenging because the clinical symptoms overlap with other neurodegenerative diseases. The discovery of reliable biomarkers is highly expected to facilitate clinical diagnosis. Through the analysis of the ¹H magnetic resonance spectroscopy (¹H-MRS) in the putamen, the purpose of the study was to discuss the possibility of the difference in metabolite concentrations between the left and right putamen as biomarkers for patients with severe PD.

Methods: We collected ¹H-MRS of unilateral or bilateral putamen from 41 patients and used the independent sample *t*-test and paired *t*-test to analyze 4 metabolite concentrations, including choline (Cho), total N-acetyl aspartate (tNAA), total creatine (tCr), and combined glutamate and glutamine; Bonferroni correction was used to correct P values for multiple comparisons. We designed 4 controlled experiments as follows: (I) PD patients versus healthy controls (HCs) in the left putamen; (II) PD patients versus HCs in the right putamen; (III) the left putamen versus the right putamen for PD patients; and (IV) the left putamen versus the right putamen for HCs.

Results: No statistically significant differences ($P>0.05$) were detected among 4 metabolites in the ipsilateral and bilateral putamen for the PD and HCs groups, except for tCr in the left putamen (PD 6.426 ± 0.557 , HCs 6.026 ± 0.460 , $P=0.046$) for ipsilateral comparisons.

Conclusions: In the bilateral putamen of severe PD patients, there was no statistically significant difference in the 4 metabolites. The difference ($P<0.05$) in tCr in the left putamen might be a potential biomarker to distinguish HCs from severe patients in clinic. This might provide a reference for the clinical diagnosis and acquisition strategy of ¹H-MRS in severe PD.

Keywords: Parkinson's disease (PD); ¹H magnetic resonance spectroscopy (¹H-MRS); metabolites; bilateral putamen

Submitted Feb 25, 2023. Accepted for publication Jul 28, 2023. Published online Aug 22, 2023.

doi: 10.21037/qims-23-231

View this article at: <https://dx.doi.org/10.21037/qims-23-231>

Introduction

Parkinson's disease (PD), which often develops after the age of 50, is a common neurodegenerative disease (1-4). PD is regarded as a movement disorder (5), with bradykinesia, tremor, rigidity, and postural instability as early symptoms, as well as some non-motor symptoms such as hyposmia, constipation, memory loss, and sleep disturbances which can worsen conditions at a later stage (2,6-8). When it comes to pathological mechanisms, the former mainly results from the loss of dopaminergic neurons in the substantia nigra pars compacta (9); however, the latter is associated with the central and autonomic nervous systems (10). The putamen, a round structure located at the bottom of the forebrain (telencephalon), functions well in PD, regulating movements at different phases (e.g., preparation and execution) and influencing different forms of learning. Specifically, patients with PD exhibit dopaminergic neuron degeneration in the substantia nigra and concurrent reductions in dopamine levels in the striatum, notably the putamen (11). Although age as the strongest risk factor for PD (9), followed by other environmental factors, such as tobacco (12) and pesticides (10), and even genetic variants have been discussed (13), the cause of PD remains unclear. Additionally, the diagnosis of PD faces challenges since PD's clinical symptoms overlap with those of other neurodegenerative diseases, and tests and biomarkers limit the reliable diagnosis at the early stage (2). Clinicopathological studies using brain bank material from the UK and Canada suggest that clinicians misdiagnose approximately 25% of patients (14).

Measuring the metabolic concentrations for PD with non-invasive and *in vivo* ^1H magnetic resonance spectroscopy (^1H -MRS) is a valuable way (15,16). Particularly, ^1H -MRS can reflect the conditions of neurons, myelin integrity, energy metabolism, and metabolically active neuro-biochemicals (17), showing great potential in PD diagnosis. Some common metabolites measured by MRS include the following: (I) choline (Cho). Composed of glycerophosphorylcholine (GPC) and phosphatidylcholine (PCh), Cho's peak shows a disorderly specific increase or decrease (18,19), by which membrane synthesis and degradation (20,21) are shown; (II) total NAA (tNAA). tNAA consists of N-acetyl aspartate (NAA) and N-Acetyl-aspartyl-glutamate (NAAG). Synthesized in neuronal

mitochondria (18), NAA is deemed a neuronal marker of which reduction is associated with neuronal loss and reduced metabolic activity (18-20,22,23). NAA reduction has been observed in some brain diseases such as brain tumor. As a peptide neurotransmitter, NAAG is used in the nervous system (20); (III) total creatine (tCr). tCr, including creatine (Cr) and phosphocreatine (PCr), plays a role in buffering and shuttling energy (20); (IV) Glx [combined glutamate (Glu) and glutamine (Gln)]. Glx is an important neurometabolite (18,21,24), the concentration of which can tend to increase in stroke, epilepsy, and neurodegenerative diseases (20). According to a study of blood biomarkers for PD, increased serum metabolic profiles such as Gln indicate abnormalities in metabolites and the tricarboxylic acid (TCA) cycle (25).

Earlier studies made great achievements in the diagnosis of PD with MRS. Some typical work has focused on distinguishing PD from healthy controls (HCs) in the same region, with the following findings: (I) A decline in striatal tCr in the striatal thalamic in patients with PD compared to HC (26); (II) Significantly low Cr in left basal ganglia in tremor-dominant PD compared with PD with postural instability and gait difficulty (27); and (III) It has been found that the NAA/Cr ratio and Cho/Cr ratio can decrease in tremor-dominant PD in the bilateral thalamus (28). Other studies have emphasized different regions: (I) A ^1H -MRS (7T) study on mild to moderate PD studied metabolite GABA+ in the pons, putamen, and substantia nigra, and found significance in the pons and putamen (24); (II) The medulla oblongata, substantia nigra, putamen, and motor cortex have also been studied before, where only NAA/Cr in substantia nigra showed significant a difference (29); (III) Another ^1H -MRS (1.5T) study found significantly different reductions in NAA/Cr in the putamen (30). However, the differences between the left and right putamen for patients with severe PD have remained unclear, which is the main focus of this work.

Methods

Participants and experimental design

The study was conducted in accordance with the Declaration of Helsinki (as revised in 2013). The study was

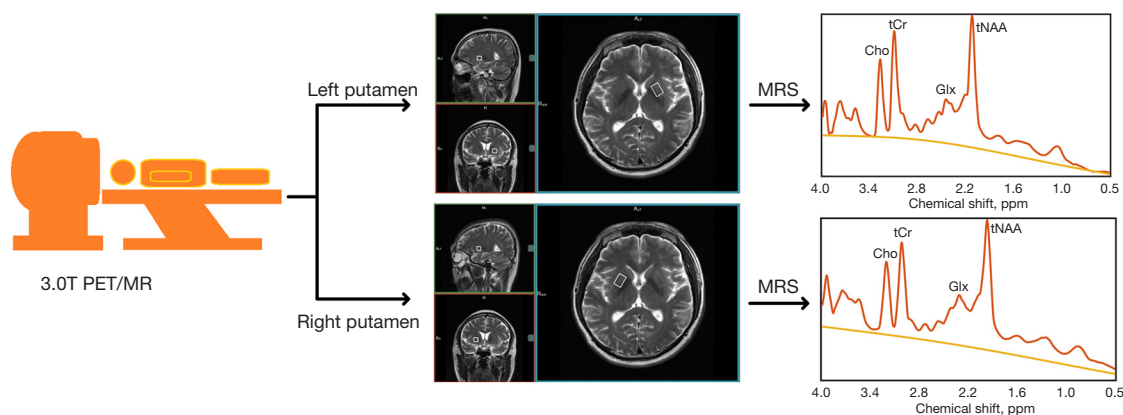


Figure 1 ¹H-MRS data collection flowchart of the study. The left and right putamen were used as regions of interest and represented by white boxes to obtain metabolite concentrations of Cho, tCr, Glx, and tNAA of participants. PET, positron emission tomography; MR, magnetic resonance; MRS, magnetic resonance spectroscopy; Cho, choline; tCr, total creatine; Glx, combined glutamate and glutamine; tNAA, total N-acetyl aspartate.

approved by the Medical Ethics Committee of the Nanjing First Hospital, and informed consent was provided by all participants. We collected ¹H-MRS data from April 2021 to May 2022. A flowchart of the single-voxel ¹H-MRS collection process is shown in *Figure 1*. A radiologist with 10 years of experience placed the region of interest (ROI) in the participants' related brain areas to obtain the metabolite concentrations of Cho, tNAA, tCr, and Glx. The actual concentration of metabolites was adopted to conduct a comparative analysis in the study; all data were presented as mean \pm standard deviation (SD) in control experiments. The study involved 41 participants, including 22 patients with severe PD (12 males and 10 females, age range: 69.36 \pm 13.38 years) and 19 HCs (12 males and 7 females, age range, 42.68 \pm 19.15 years). A total of 13 patients with PD were tested on the bilateral putamen, 5 patients with PD were tested on the left putamen, and 4 patients with PD were tested on the right putamen, and 8 HCs were tested on the bilateral putamen and 11 HCs were tested on the left putamen with a hybrid 3.0T positron emission tomography and magnetic resonance (PET/MR) imaging scanner produced by United Imaging (Shanghai, China).

The specific procedure for PD comprised 2 steps: (I) The neurologist ascertained whether the patient was afflicted with Parkinson's syndrome, namely, bradykinesia and at least 1 of 2 principal signs which are static tremor and rigidity. Then, all the core principal signs were examined using the procedures outlined in the MDS-Unified Parkinson's Disease Rating Scale (MDS-UPDRS). (II) When Parkinson's syndrome was identified, these

criteria were used to make a definite diagnosis of PD: (i) not meeting absolute exclusion criteria; (ii) having at least 2 supportive criteria; and (iii) no red flags such as severe autonomic dysfunction within 5 years of development. Reference was made to the Diagnostic Criteria for Parkinson's Disease in China (2016) (31), specifically, the following exclusion criteria: (I) unequivocal cerebellar abnormalities, such as cerebellar gait, limb ataxia, or cerebellar oculomotor abnormalities; (II) downward vertical supranuclear gaze palsy, or selective saccade slowing in the downward direction; (III) Parkinsonian symptoms limited to the lower limbs had been present for 3 years or longer; (IV) unequivocal cortical sensory loss, unmistakable limb ideomotor apraxia, or progressive aphasia; (V) usual functional neuroimaging of the presynaptic dopaminergic system. Supportive criteria included the following: (I) clear and dramatic positive response to dopaminergic therapy; (II) existence of levodopa-induced dyskinesia; (III) limb resting tremor recorded on clinical examination; (IV) the existence of either olfactory loss or cardiac sympathetic denervation on metaiodobenzylguanidine scintigraphy. Patients with clinical disability at Hoehn-Yahr (32) stage III and above were classified as having severe PD.

Data preprocessing was applied first, and the specific process was as follows: raw data processing channels merger, motion correction, phase and frequency alignment, and eddy current correction. LCmodel (Provencher; <http://s-provencher.com/lcmodel.shtml>) was used to quantify metabolites, and the basis set uses `press_te30_3t_v3`, which is generated from measured data and provided

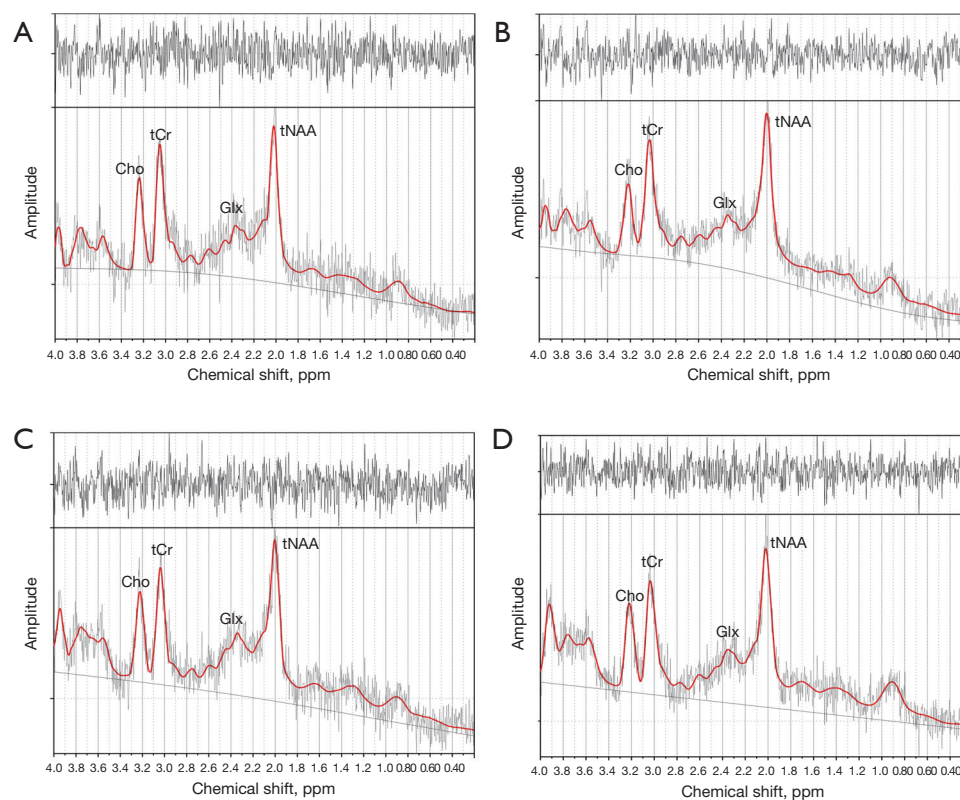


Figure 2 ^1H -MRS of bilateral putamen for healthy volunteers and patients. (A,B) The ^1H -MRS of a volunteer's left and right putamen, respectively. (C,D) The ^1H -MRS of left and right putamen of a PD patient, respectively. MRS, magnetic resonance spectroscopy; PD, Parkinson's disease; Cho, choline; tCr, total creatine; Glx, combined glutamate and glutamine; tNAA, total N-acetyl aspartate.

by Provencher (source: <http://s-provencher.com/lcm-basis.shtml>). The unsuppressed water spectrum was used to estimate metabolite concentrations (28), and the quantification results obtained by LCModel are shown in *Figure 2*.

The following 4 control experiments were designed: (I) PD versus HCs in the left putamen: 18 PD (10 males and 8 females) and 19 HC (12 males and 7 females); (II) PD versus HCs in the right putamen: 17 PD (10 males and 7 females) and 8 HC (4 males and 4 females); (III) the left putamen versus the right putamen for PD: 13 PD (8 males and 5 females); and (IV) the left putamen versus the right putamen for HCs: 8 HCs (4 males and 4 females). It should be noted that the final 2 experiments compared bilateral putamen metabolite concentrations from the same participant.

^1H -MRS parameter setting

^1H -MRS was acquired on a hybrid 3.0T PET/MR scanner

(uPMR790; United-Imaging Healthcare) with a 32-channel head/neck coil using *svs_press* sequence, with the following parameters: repetition time (TR) = 2,000 ms; echo time (TE) = 30 ms; flip angle = 90°; chemical shift = 2.0 ppm; bandwidth = 4,000 Hz/px; orientation = transversal (T); number of signal-averaged (NSA) = 128; volume of interest (VOI) = 10 × 10 × 15 mm³ (*Table 1*).

Statistical methods

The metabolite concentrations (Cho, tNAA, tCr, and Glx) determined by ^1H -MRS were analyzed using SPSS statistical software (version 22.0; IBM Corp., Armonk, NY, USA). Independent sample *t*-test and the paired *t*-test were used to analyze the metabolite concentrations, and Bonferroni correction was used to correct P values for multiple comparisons. The independent samples *t*-test was employed in the PD versus HCs group in the left and right putamen. On account of the data pairing, the paired *t*-test was used to compare the left and right putamen of the PD

Table 1 Imaging parameters of 3.0T PET/MR scanner

Parameters	Values
TR (ms)	2,000
TE (ms)	30
Flip angle (°)	90
Chemical shift (ppm)	2.0
Bandwidth (Hz/px)	4,000
Orientation	Transversal (T)
Number of signal averaged	128
VOI (mm ³)	10×10×15
Coil number	32

PET, positron emission tomography; MR, magnetic resonance; TR, repetition time; TE, echo time; VOI, volume of interest.

and HCs groups. Statistical significance was considered if $P < 0.05$.

Results

The 4 controlled experiments were designed as follows: (I) PD versus HCs in the left putamen; (II) PD versus HCs in the right putamen; (III) the left putamen versus the right putamen for PD; and (IV) the left putamen versus the right putamen for HCs. The quantitative results of MRS are shown in *Figure 3*.

In the left putamen: PD versus HCs

Compared with the HCs (*Table 2*), 4 metabolite concentrations (Cho, tNAA, tCr, and Glx) were higher in the PD group in the left putamen. As shown in *Figure 3A* and *Table 2*, 3 metabolite concentrations (Cho, tNAA, and Glx) were not statistically different in the PD and HCs groups. The only metabolite with a statistically significant difference ($P < 0.05$) was tCr (PD 6.426 ± 0.557 , HCs 6.026 ± 0.460 , $P = 0.046$).

In the right putamen: PD versus HCs

The results (*Table 3*) indicated that 2 metabolite concentrations including Cho and tNAA in the PD group were lower than those in HCs in the right putamen. As *Table 3* and *Figure 3B* depict, all metabolite concentrations were not statistically different in the PD group as well as in

HCs (Cho: PD 1.894 ± 0.295 , HCs 2.063 ± 0.333 , $P = 0.486$; tNAA: PD 7.049 ± 0.674 , HCs 7.198 ± 1.330 , $P = 0.999$; tCr: PD 6.509 ± 0.737 , HCs 6.411 ± 0.775 , $P = 0.999$; Glx: PD 11.140 ± 2.213 , HCs 11.000 ± 1.634 , $P = 0.999$).

PD: the left putamen versus the right putamen

When it referred to PD's bilateral putamen, some distinctions between the left and right putamen were observed, as displayed in *Table 4* and *Figure 3C*. Cho and Glx were higher in the left putamen than those in the right putamen. However, tCr was found to be lower in the left putamen than that in the right putamen. All of the metabolite concentrations were not statistically different between the left putamen and the right putamen for PD (Cho: left 2.087 ± 0.248 , right 1.868 ± 0.309 , $P = 0.062$; tNAA: left 6.925 ± 0.756 , right 6.978 ± 0.607 , $P = 0.999$; tCr: left 6.546 ± 0.528 , right 6.459 ± 0.619 , $P = 0.999$; Glx: left 12.302 ± 1.710 , right 11.122 ± 2.511 , $P = 0.404$).

HCs: the left putamen versus the right putamen

Table 5 illustrates that Cho was higher in the left putamen than it was in the right putamen in the HC group. Besides, all metabolite concentrations, including Cho, tNAA, tCr, and Glx, showed no statistical difference in *Figure 3D* (Cho: left 2.116 ± 0.226 , right 2.063 ± 0.118 , $P = 0.999$; tNAA: left 6.699 ± 0.721 , right 7.198 ± 1.330 , $P = 0.557$; tCr: left 6.078 ± 0.492 , right 6.411 ± 0.775 ; $P = 0.523$; Glx: left 11.431 ± 1.040 , right 11.001 ± 1.634 , $P = 0.999$).

Discussion

In this study, 4 metabolites, including Cho, tNAA, tCr, and Glx, were analyzed using MRS. Compared with HCs, all metabolite concentrations increased in the left putamen for the PD group (*Table 2*, Cho: PD 2.026 ± 0.236 , HCs 1.834 ± 0.311 ; tNAA: PD 6.951 ± 0.646 , HCs 6.478 ± 0.831 ; tCr: PD 6.426 ± 0.557 , HCs 6.026 ± 0.460 ; Glx: PD 12.087 ± 1.683 , HCs 11.250 ± 1.359). Contrastingly, Cho (*Table 3*, PD: 1.894 ± 0.295 , HCs: 2.063 ± 0.333) and tNAA (PD: 7.049 ± 0.674 , HCs: 7.198 ± 1.330) decreased in the right putamen in the PD group. These findings were consistent with those of previous investigations (28,33). In particular, reduced tNAA might be caused by neuronal loss or degeneration in PD patients, as well as mitochondrial dysfunction in the brain. The decreased Cho might be explained by a relationship between the neurodegenerative

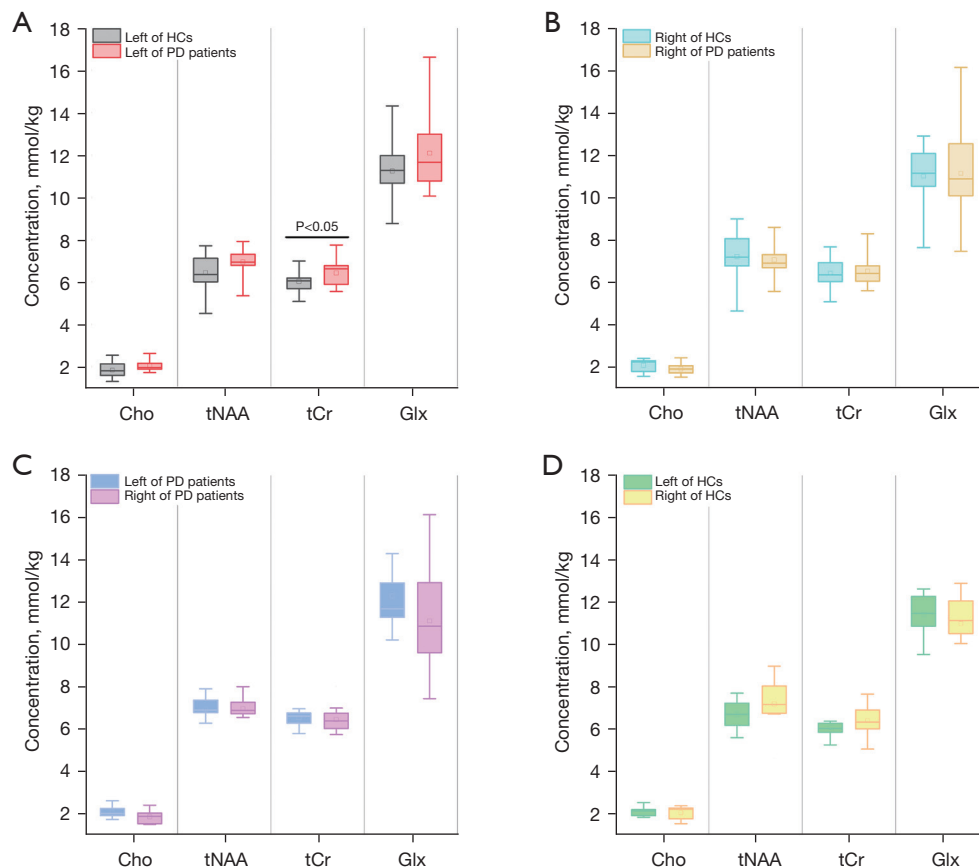


Figure 3 Box plots of four metabolite concentrations in control experiments. (A) The comparisons in metabolite concentrations between PD and HCs in the left putamen. (B) The comparisons in metabolite concentrations between PD and HCs in the right putamen. (C) The comparisons in metabolite concentrations between the left and the right putamen for PD. (D) The comparisons in metabolite concentrations between the left and the right putamen for HCs. HCs, healthy controls; PD, Parkinson’s disease; Cho, choline; tNAA, total N-acetyl aspartate; tCr, total creatine; Glx, combined glutamate and glutamine.

Table 2 Comparisons between PD and HCs in the left putamen

Metabolite ratio	PD	HCs	P value
Cho	2.026±0.236	1.834±0.311	0.083
tNAA	6.951±0.646	6.478±0.831	0.086
tCr	6.426±0.557	6.026±0.460	0.046*
Glx	12.087±1.683	11.250±1.359	0.214

The data were presented as mean ± standard deviation. *, P<0.05 is statistically significant. PD, Parkinson’s disease; HCs, healthy controls; Cho, choline; tNAA, total N-acetyl aspartate; tCr, total creatine; Glx, combined glutamate and glutamine.

Table 3 Comparisons between PD and HCs in the right putamen

Metabolite ratio	PD	HCs	P value
Cho	1.894±0.295	2.063±0.333	0.486
tNAA	7.049±0.674	7.198±1.330	0.999
tCr	6.509±0.737	6.411±0.775	0.999
Glx	11.140±2.213	11.000±1.634	0.999

The data were presented as mean ± standard deviation. PD, Parkinson’s disease; HCs, healthy controls; Cho, choline; tNAA, total N-acetyl aspartate; tCr, total creatine; Glx, combined glutamate and glutamine.

Table 4 Comparisons between the left and the right putamen for PD

Metabolite ratio	Left	Right	P value
Cho	2.087±0.248	1.868±0.309	0.062
tNAA	6.925±0.756	6.978±0.607	0.999
tCr	6.546±0.528	6.459±0.619	0.999
Glx	12.302±1.710	11.122±2.511	0.404

The data were presented as mean ± standard deviation. PD, Parkinson's disease; Cho, choline; tNAA, total N-acetyl aspartate; tCr, total creatine; Glx, combined glutamate and glutamine.

Table 5 Comparisons between the left and the right putamen for HCs

Metabolite ratio	Left	Right	P value
Cho	2.116±0.226	2.063±0.118	0.999
tNAA	6.699±0.721	7.198±1.330	0.557
tCr	6.078±0.492	6.411±0.775	0.523
Glx	11.431±1.040	11.001±1.634	0.999

The data were presented as mean ± standard deviation. HCs, healthy controls; Cho, choline; tCr, total creatine; tNAA, total N-acetyl aspartate; Glx, combined glutamate and glutamine.

process and defects of cholesterol metabolism in the plasma membranes of neurons and glial cells and the myelin membranes (34). We found different trends in the concentrations of metabolites in the left and right putamen, which may be due to the asymmetry of the bilateral putamen (30).

The independent samples *t*-test was used to compare the differences in metabolite concentrations in the ipsilateral putamen between the PD and HC groups. The results indicated that both Cho and tNAA increased in the left putamen whereas they decreased in the right putamen, showing opposite trends in the PD and HCs groups, and 3 metabolites concentrations (Cho, tNAA, and Glx) had no significant difference (Table 2 and Table 3). There was 1 metabolite concentration tCr that was statistically significant in the left putamen (Table 2, tCr: PD 6.426±0.557, HCs 6.026±0.460, P=0.046) between the PD group and HCs rather than in the right putamen (Table 3, tCr: PD 6.509±0.737, HCs 6.411±0.775, P=0.999). Overall, when comparing the PD and HCs groups, both left and right putamen showed approximately the same statistical regularity, namely, no significant difference for

3 metabolites (Cho, tNAA, and Glx). The tCr may be a potential biomarker when MRS is used to identify patients with severe PD.

As shown in Table 4 and Table 5, the paired *t*-test was adopted to test whether some metabolite concentrations might exist in statistical differences in the bilateral putamen between the PD and HCs groups. When it comes to metabolite concentrations in the bilateral putamen, higher metabolite concentrations including Cho, tNAA, and Glx in the left putamen for the PD group (Table 4, Cho: left 2.087±0.248, right 1.868±0.309; tNAA: left 6.925±0.756, right 6.978±0.607; Glx: left 12.302±1.710, right 11.122±2.511) were observed, whereas the sole metabolite Cho was elevated in the left putamen for the HCs group (Table 5, Cho: left 2.116±0.226, right 2.063±0.118). tNAA was used as a potential biomarker for the diagnosis of PD, and its concentration was similar in bilateral putamen in the PD group (Table 4, left: 6.925±0.756 right: 6.978±0.607), suggesting that the acquisition of either the left or right putamen might not result in significant changes in tNAA (35). Besides, for the PD group, 4 concentrations including Cho, tNAA, tCr, and Glx showed no significant difference in the bilateral putamen (Table 4, Cho: P=0.062; tNAA: P=0.999; tCr: P=0.999; Glx: P=0.404), which was consistent with the findings of the bilateral lentiform nucleus, midbrain, white matter of frontal lobe, and hippocampus without significant changes (35). This may be due to bilateral striatal neuronal damage in patients with severe PD, which manifests as bilateral limb movement involvement (32,36). Similarly, the HCs group showed the same results, for which all metabolite concentrations had no statistically significant difference (Table 5, Cho: P=0.999; tNAA: P=0.557; tCr: P=0.523; Glx: P=0.999). The conclusions indicated that there was no statistical difference in bilateral putamen in patients with severe PD.

There were some highlights distinguishing our work from earlier studies. First, unlike most previous studies that used stable Cr as the denominator of metabolite ratios (21), our work adopted actual concentrations for control experiments since tCr was found to be variable in PD (Table 2 and Table 3, left putamen: 6.426±0.557, right putamen: 6.509±0.737), which might reduce the analysis error. This might also provide an effective analysis strategy for the diagnosis of PD using MRS on the putamen in the future. Additionally, we studied the metabolite concentration differences in bilateral putamen of PD patients whereas others had focused on single or multiple regions where the putamen was seldomly analyzed between

the PD and HC groups. Although there existed some bilateral studies, the regions were substantia nigra, thalamus, and so on, rather than putamen. To our knowledge, no other work has involved studies of bilateral differences in the concentration of metabolites in the putamen.

Some limitations were noted in the study. First, some advanced MRS quantification techniques which might increase the accuracy of MRS analysis were not adopted. Specifically, previous research has recommended the semi-adiabatic LASER sequence, which can overcome some limitations such as localization error (37). Besides, the built-in macromolecule was used instead of the measured macromolecule, which might have led to minor bias in some metabolites. In future work, one could try to use measured mobile macromolecules, which not only reduce bias but also serve as biomarkers for certain diseases (38). Finally, the sample size of HCs should be increased to statistically match that of PD.

Conclusions

To discuss the possibility of the difference in metabolite concentrations between the bilateral putamen as biomarkers in severe PD patients, 4 controlled experiments were designed. The results showed that no statistically significant differences existed among all metabolite concentrations (Cho, tNAA, tCr, and Glx) in the ipsilateral and bilateral putamen for the PD and HCs group ($P > 0.05$), except for tCr ($P < 0.05$) in the left putamen for ipsilateral comparisons. Therefore, in the bilateral putamen of severe PD patients, there was no statistically significant difference in the 4 metabolites (Cho, tNAA, tCr, and Glx). The difference in tCr in the left putamen might be a potential biomarker to distinguish HCs from severe patients clinically. This might provide a reference for the clinical diagnosis and acquisition strategy of ^1H -MRS in severe PD.

Acknowledgments

This work was supported by the Nanjing First Hospital.

Funding: This study was partially supported by the National Natural Science Foundation of China (Nos. 62122064 and 61971361), President Fund of Xiamen University (No. 20720220063), and Xiamen University Nanqiang Outstanding Talents Program.

Footnote

Conflicts of Interest: All authors have completed the ICMJE uniform disclosure form (available at <https://qims.amegroups.com/article/view/10.21037/qims-23-231/coif>). HS is a current employee of the United Imaging Research Institute of Intelligent Imaging, Beijing, China. The other authors have no conflicts of interest to declare.

Ethical Statement: The authors are accountable for all aspects of the work in ensuring that questions related to the accuracy or integrity of any part of the work are appropriately investigated and resolved. The study was conducted in accordance with the Declaration of Helsinki (as revised in 2013). The study was approved by the Medical Ethics Committee of the Nanjing First Hospital, and informed consent was provided by all participants.

Open Access Statement: This is an Open Access article distributed in accordance with the Creative Commons Attribution-NonCommercial-NoDerivs 4.0 International License (CC BY-NC-ND 4.0), which permits the non-commercial replication and distribution of the article with the strict proviso that no changes or edits are made and the original work is properly cited (including links to both the formal publication through the relevant DOI and the license). See: <https://creativecommons.org/licenses/by-nc-nd/4.0/>.

References

1. Bloem BR, Okun MS, Klein C. Parkinson's disease. *Lancet* 2021;397:2284-303.
2. Tolosa E, Garrido A, Scholz SW, Poewe W. Challenges in the diagnosis of Parkinson's disease. *Lancet Neurol* 2021;20:385-97.
3. He C, Rong S, Zhang P, Li R, Li X, Li Y, Wang L, Zhang Y. Metabolite changes in prefrontal lobes and the anterior cingulate cortex correlate with processing speed and executive function in Parkinson disease patients. *Quant Imaging Med Surg* 2022;12:4226-38.
4. Salmanpour MR, Shamsaei M, Hajianfar G, Soltanian-Zadeh H, Rahmim A. Longitudinal clustering analysis and prediction of Parkinson's disease progression using radiomics and hybrid machine learning. *Quant Imaging Med Surg* 2022;12:906-19.

5. Kurtis MM, Pareés I. Functional movement disorder comorbidity in Parkinson's disease: Unraveling the web. *Parkinsonism Relat Disord* 2021;82:138-45.
6. Jankovic J. Pathophysiology and clinical assessment of Parkinsonian symptoms and signs. In: Pahwa R, Lyons KE. Editors. *Handbook of Parkinson's disease*. 3rd edition. CRC Press; 2003:90-127.
7. Rong S, Li Y, Li B, Nie K, Zhang P, Cai T, Mei M, Wang L, Zhang Y. Meynert nucleus-related cortical thinning in Parkinson's disease with mild cognitive impairment. *Quant Imaging Med Surg* 2021;11:1554-66.
8. Xu R, Hu X, Jiang X, Zhang Y, Wang J, Zeng X. Longitudinal volume changes of hippocampal subfields and cognitive decline in Parkinson's disease. *Quant Imaging Med Surg* 2020;10:220-32.
9. Driver JA, Logroscino G, Gaziano JM, Kurth T. Incidence and remaining lifetime risk of Parkinson disease in advanced age. *Neurology* 2009;72:432-8.
10. Costello S, Cockburn M, Bronstein J, Zhang X, Ritz B. Parkinson's disease and residential exposure to maneb and paraquat from agricultural applications in the central valley of California. *Am J Epidemiol* 2009;169:919-26.
11. Dal Ben M, Bongiovanni R, Tuniz S, Fioriti E, Tiribelli C, Moretti R, Gazzin S. Earliest Mechanisms of Dopaminergic Neurons Sufferance in a Novel Slow Progressing Ex Vivo Model of Parkinson Disease in Rat Organotypic Cultures of Substantia Nigra. *Int J Mol Sci* 2019;20:2224.
12. Hernán MA, Takkouche B, Caamaño-Isorna F, Gestal-Otero JJ. A meta-analysis of coffee drinking, cigarette smoking, and the risk of Parkinson's disease. *Ann Neurol* 2002;52:276-84.
13. Blauwendraat C, Nalls MA, Singleton AB. The genetic architecture of Parkinson's disease. *Lancet Neurol* 2020;19:170-8.
14. Tolosa E, Wenning G, Poewe W. The diagnosis of Parkinson's disease. *Lancet Neurol* 2006;5:75-86.
15. Salari S, Bagheri M. In vivo, in vitro and pharmacologic models of Parkinson's disease. *Physiol Res* 2019;68:17-24.
16. Almuqbel M, Melzer TR, Myall DJ, MacAskill MR, Pitcher TL, Livingston L, Wood KL, Keenan RJ, Dalrymple-Alford JC, Anderson TJ. Metabolite ratios in the posterior cingulate cortex do not track cognitive decline in Parkinson's disease in a clinical setting. *Parkinsonism Relat Disord* 2016;22:54-61.
17. Chaudhary S, Kumari S, Kumaran SS, Goyal V, Jain S, Kaloiya GS. In vitro and in vivo NMR based metabolomics in Parkinson's disease. *J Magn Reson Open* 2022;10-11:100050.
18. van der Graaf M. In vivo magnetic resonance spectroscopy: basic methodology and clinical applications. *Eur Biophys J* 2010;39:527-40.
19. Ding XQ, Maudsley AA, Sabati M, Sheriff S, Schmitz B, Schütze M, Bronzlik P, Kahl KG, Lanfermann H. Physiological neuronal decline in healthy aging human brain - An in vivo study with MRI and short echo-time whole-brain (1)H MR spectroscopic imaging. *Neuroimage* 2016;137:45-51.
20. Henning A. In vivo 1H MRS applications. In: Lindon JC. editor. *Encyclopedia of Spectroscopy and Spectrometry*. 2nd edition. Oxford: Elsevier; 2010:1077-84.
21. Hammen T, Kuzniecky R. Magnetic resonance spectroscopy in epilepsy. *Handb Clin Neurol* 2012;107:399-408.
22. Hetherington H, Petroff O, Jackson GD, Kuzniecky RI, Briellmann RS, Wellard RM. Magnetic resonance spectroscopy. In: Kuzniecky RI, Jackson JD. editors. *Magnetic Resonance in Epilepsy*. 2nd edition. Elsevier; 2005:333-83.
23. Petroff OA, Errante LD, Kim JH, Spencer DD. N-acetyl-aspartate, total creatine, and myo-inositol in the epileptogenic human hippocampus. *Neurology* 2003;60:1646-51.
24. Emir UE, Tuite PJ, Öz G. Elevated pontine and putamenal GABA levels in mild-moderate Parkinson disease detected by 7 tesla proton MRS. *PLoS One* 2012;7:e30918.
25. Kumari S, Kumaran SS, Goyal V, Bose S, Jain S, Dwivedi SN, Srivastava AK, Jagannathan NR. Metabolomic analysis of serum using proton NMR in 6-OHDA experimental PD model and patients with PD. *Neurochem Int* 2020;134:104670.
26. Pesch B, Casjens S, Woitalla D, Dharmadhikari S, Edmondson DA, Zella MAS, Lehnert M, Lotz A, Herrmann L, Muhlack S, Kraus P, Yeh CL, Glaubitz B, Schmidt-Wilcke T, Gold R, van Thriel C, Brüning T, Tönges L, Dydak U. Impairment of Motor Function Correlates with Neurometabolite and Brain Iron Alterations in Parkinson's Disease. *Cells* 2019;8:96.
27. Gong T, Xiang Y, Saleh MG, Gao F, Chen W, Edden RAE, Wang G. Inhibitory motor dysfunction in parkinson's disease subtypes. *J Magn Reson Imaging* 2018;47:1610-5.
28. Barbagallo G, Arabia G, Morelli M, Nisticò R, Novellino F, Salsone M, Rocca F, Quattrone A, Caracciolo M, Sabatini U, Cherubini A, Quattrone A. Thalamic neurometabolic alterations in tremulous Parkinson's disease: A preliminary proton MR spectroscopy study. *Parkinsonism Relat Disord*

- 2017;43:78-84.
29. Cao H, Shi J, Cao B, Kang B, Zhang M, Qu Q. Evaluation of the Braak staging of brain pathology with (1)H-MRS in patients with Parkinson's disease. *Neurosci Lett* 2017;660:57-62.
 30. Abe K, Terakawa H, Takanashi M, Watanabe Y, Tanaka H, Fujita N, Hirabuki N, Yanagihara T. Proton magnetic resonance spectroscopy of patients with parkinsonism. *Brain Res Bull* 2000;52:589-95.
 31. Chinese Medical Association Neurology Branch Parkinson's Disease and Movement Disorders Study Group; Chinese Medical Doctor Association Neurology Branch Parkinson's Disease and Movement Disorders Specialty. Diagnostic criteria of Parkinson's disease in China (2016 edition). *Chinese Journal of Neurology* 2016;49:268-71.
 32. Goetz CG, Poewe W, Rascol O, Sampaio C, Stebbins GT, Counsell C, Giladi N, Holloway RG, Moore CG, Wenning GK, Yahr MD, Seidl L; . Movement Disorder Society Task Force report on the Hoehn and Yahr staging scale: status and recommendations. *Mov Disord* 2004;19:1020-8.
 33. Gröger A, Kolb R, Schäfer R, Klose U. Dopamine reduction in the substantia nigra of Parkinson's disease patients confirmed by in vivo magnetic resonance spectroscopic imaging. *PLoS One* 2014;9:e84081.
 34. Guan J, Rong Y, Wen Y, Wu H, Qin H, Zhang Q, Chen W. Detection and application of neurochemical profile by multiple regional (1)H-MRS in Parkinson's disease. *Brain Behav* 2017;7:e00792.
 35. Saeed U, Lang AE, Masellis M. Neuroimaging Advances in Parkinson's Disease and Atypical Parkinsonian Syndromes. *Front Neurol* 2020;11:572976.
 36. Farombi EO, Awogbindin IO, Farombi TH, Oladele JO, Izomoh ER, Aladelokun OB, Ezekiel IO, Adebambo OI, Abah VO. Neuroprotective role of kolaviron in striatal redo-inflammation associated with rotenone model of Parkinson's disease. *Neurotoxicology* 2019;73:132-41.
 37. Öz G, Deelchand DK, Wijnen JP, Mlynárik V, Xin L, Mekle R, Noeske R, Scheenen TWJ, Tkáč I; . Advanced single voxel (1) H magnetic resonance spectroscopy techniques in humans: Experts' consensus recommendations. *NMR Biomed* 2020. [Epub ahead of print]. doi: 10.1002/nbm.4236.
 38. Cudalbu C, Behar KL, Bhattacharyya PK, Bogner W, Borbath T, de Graaf RA, et al. Contribution of macromolecules to brain (1) H MR spectra: Experts' consensus recommendations. *NMR Biomed* 2021;34:e4393.

Cite this article as: Qu B, Li X, Xiao M, Chen R, Tan H, Sun H, Li R, Xu J, Dong J, Zheng G, Ai S, Qu X. Comparative study of bilateral putamen for patients with severe Parkinson's disease detected by 1H magnetic resonance spectroscopy. *Quant Imaging Med Surg* 2023;13(10):6646-6655. doi: 10.21037/qims-23-231